AENSI Journals

Australian Journal of Basic and Applied Sciences

ISSN:1991-8178

Journal home page: www.ajbasweb.com

Comparison of Current Control Schemes for a Three Phase Grid Connected PV Systems with MPPT

[1]G. Parameswari Ganesan and [2]Dr. R. Arumugam

[1] *Research Scholar, Dept. of EEE, S.S.N College Of Engineering, Kalavakkam - 603 110, Chennai, India*
[2] *Professor, Dept. of EEE, S.S.N College Of Engineering, Kalavakkam - 603 110, Chennai, India*

ARTICLE INFO

Article history:
Received 10 October 2014
Received in revised form
22 November 2014
Accepted 28 November 2014
Available online 1 December 2014

Keywords:
Photovoltaic (PV); Maximum Power Point Tracking (MPPT); Pulse Width Modulated (PWM); Voltage Source Inverter (VSI); Sliding Mode Control (SMC); Unity Power Factor (UPF)

ABSTRACT

This paper compares three different types of inner loop current control strategy for three-phase grid connected photovoltaic (PV) system with maximum power point tracking (MPPT). The three phase PWM rectifier topology is operated in inverter mode. Perturb and Observe algorithm is used to track the maximum power point (MPP), resulting in a reference voltage that is in turn used for reference current generation. PWM rectifier feeding power to grid is effectively controlled by comparing the actual and reference currents. The outer capacitor voltage control loop uses a PI regulator and the different current control techniques taken up for inner current control loop to compare are Hysteresis, Sliding Mode Control and Linear Current Control. The entire system is modeled and simulated using Matlab. Single stage grid connected Photovoltaic (PV) systems avoids complex topologies leading to high efficiencies. The objective is to choose a simple technique that draws maximum power from PV source and injects to grid at Unity Power Factor.

To Cite This Article: G. Parameswari Ganesan and Dr. R. Arumugam., Comparison of Current Control Schemes for a Three Phase Grid Connected PV Systems with MPPT. ***Aust. J. Basic & Appl. Sci.,*** *8(18): 299-310, 2014*

INTRODUCTION

The interest in solar power has been rapidly growing due to its direct electric power form; little maintenance; no noise and pollution. Solar power uses the photovoltaic (PV) effect to convert incident solar energy into electrical energy. Power electronics technology efficiently processes electric power and plays an important role in effectively integrating distributed generation units providing better efficiency and performance of the power systems (Blaabjerg *et al*, 2004).

The hierarchy of PV systems varies from the past centralized scheme to the present day string inverters and modular inverter technology (Carrasco *et al*, 2006). The centralized scheme has undergone many modifications either by its topology of transformer less PV fed grid tied inverter (Yunjie Gu *et al*, 2013 and Alajmi *et al*, 2013) or in its control of grid-side inverter (Blaabjerg *et al*, 2006, Wu Libo *et al*, 2007 and Herràn *et al*, 2013).

Transformer less PV systems are achieved by the concept of virtual dc bus to eliminate the common-mode leakage current (Yunjie Gu *et al*) and also by sparingly dealt current source inverter-based photovoltaic system (Alajmi *et al*, 2013). Attempts had been made to compensate the reactive power for local load so as to alleviate grid burden (Wu Libo *et al*, 2007) and also to compensate the dead-time disturbance that leads to current distortion at zero-crossing points (Herràn *et al*, 2013).

The control strategy applied to the grid inverter consists of a fast internal current loop, that regulates the grid current, and an external voltage loop, which controls the dc-link voltage. The current loop is responsible for current wave shaping issues and current protection. The current controller major duty is to help in decreasing the current distortion by providing harmonic compensation. The voltage controller controls the dc-link voltage by balancing the power flow in the system. This controller is usually designed to provide system stability having slow dynamics (Blaabjerg *et al*, 2006).

In this work three different types of inner loop current control are compared. The three phase PWM rectifier topology is operated in inverter mode (Rodriguez *et al*, 2005) feeding power to grid at unity power factor (UPF). Of all the MPPT techniques (Esram *et al*, 2007) Perturb and Observe method is used to track the maximum power point (MPP), giving the voltage reference to control the DC bus voltage and thus forms the basis for the reference current generation. This outer capacitor voltage control loop uses a PI regulator. The inner current control loop takes up three different concepts to compare, they are Hysteresis Control (Rashid, 2001), Sliding

Corresponding Author: G. Parameswari Ganesan, Research Scholar, Dept. of EEE, S.S.N College Of Engineering, Kalavakkam - 603 110, Chennai, India.
E-mail: param_gopi2000@yahoo.com

Australian Journal of Basic and Applied Sciences, 8(18) December 2014, Pages: 299-310

Mode Control (Young *et al*, 1999, Negroni *et al*, 2010, Dannehl *et al*, 2009) and Linear Current Control (Gopalkumar). The entire system is modelled (Gonzalez-Longatt, 2005, Rusong Wu *et al*, 1990 and 1991) and simulated using Matlab. The objective is to choose a simple technique that draws maximum power from PV source and injects to grid at Unity Power Factor.

System Topology For Single Stage Grid Connected Pv System:

The solar power generation topology considered is shown in Fig. 1, wherein a PV module is connected to grid through a three phase PWM rectifier (voltage source converter). The power from PV module is supplied to the grid, when the instantaneous output voltage of the PV module exceeds the grid voltage. PWM rectifier is operated in inversion mode in such a manner (by phase shifting the reference template by 180°) that power is transferred from PV to supply grid. The objective of the work is to transfer maximum energy generated from PV to the grid at UPF. The detailed characteristics of each section are discussed in the following sections.

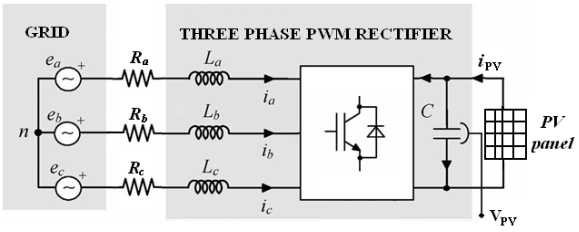

Fig. 1: Single Stage Solar Power Generation System.

A. Photovoltaic Array:

The mathematical modeling equations of the PV cells are derived from an equivalent simplified electric circuit presented in Fig. 2. As seen it consists of a voltage controlled current source, variant to two input parameters, that is, temperature (°C) and solar irradiation power (W/m^2).

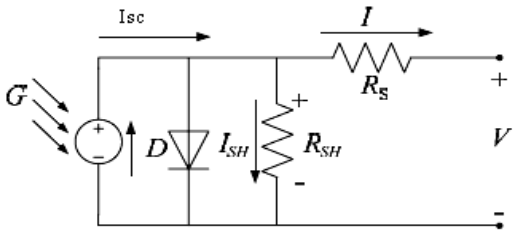

Fig. 2: Circuit diagram of PV model.

The accuracy of the model depends on the following factors (Gonzalez-Longatt, 2005).

- Temperature dependence of photo generated current I_{sc} and diode saturation current I_o.
- Irradiation dependence of photo generated current I_{sc}.
- Series resistance R_s, choice that accounts to the shape between the MPP and the open circuit voltage. This represents the internal losses due to current flow.
- Shunt resistance R_{sh} in parallel with diode, this corresponds to leakage current to ground and is commonly neglected.
- Diode ideality factor n is a variable and typically ranges between 1 and 2.

Rs and Rsh are considered to be zero for an ideal cell and the net current I of the PV cell is the derived considering the nodal equation involving photo generated current I_{sc} and diode current I_d.

$$I = I_{sc} - I_o(e^{\left(\frac{q*v_d}{n*k*T}\right)} - 1) \quad (1)$$

where

I_o is the reverse saturation current of the diode,
q is the electron charge (1.602 *10-23C),
v_d is the voltage across the diode,
k is the Boltzmann constant (1.381*10-23 J/k),
T is the junction temperature in Kelvin (K).
The model included temperature dependence of photo current I_{sc}_I_T is given by

$$I_{sc}\_I_T = I_{sc}\_I_{Tref} * \left(1 + a * \left(T - T_{ref}\right)\right) \quad (2)$$

where $I_{sc}\_I_{Tref}$ is found on datasheet (measured under irradiance of 1000W/m^2), a is the temperature coefficient of I_{sc} in percentage change per degree. The photon generated current at given irradiance is given by

$$I_{sc}\_I_G = I_{sc}\_I_{Go} * \left(\frac{G}{G_o}\right) \quad (3)$$

where G_0 is the solar irradiation of 1000W/m^2. The diode saturation current at reference temperature is given by

$$I_o(T) = I_o\left(T_{ref}\right) * \left(\frac{T}{T_{ref}}\right)^{\left(\frac{3}{n}\right)} * e - \left(\frac{q * v_d}{n * K * T}\right) * \left(\frac{1}{T - 1/T_{ref}}\right) \quad (4)$$

Eqn (1) is solved using Newton's raphson method, given by

$$x_{n+1} = x_n - \frac{f\left(x_n\right)}{f^1\left(x_n\right)} \quad (5)$$

Table 1 provides the modelling parameters for the 50W PV panel.

Table I: Specification of PV module QC50.

Sl.no	Electrical characteristics	SPI-Sun Simulator 460i Panel (QC50)
1	Maximum power (p_{max})	50W
2	Voltage at P_{max} (V_{mp})	17.82 V
3	Current at P_{max}(I_{mp})	2.84 A
4	Short circuit current (I_{sc})	2.99A
5	Open circuit voltage V_{oc}	21.6V
6	Temperature coefficient of I_{SC}	+0.05%/K
7	Temperature coefficient of V_{SC}	-0.34%/K
8	Temperature coefficient of power	-0.43%/K

B. PWM Rectifier in Inversion Mode:

The PWM rectifier is a VSI (Fig. 3) operated by maintaining the DC link voltage at a desired reference value, using a feedback control loop. The power exchanges taking place with the AC source, is based on the requirement of DC link VPV measured at the capacitor C. When the current through capacitor C is negative (inverter operation) it is charged, and this power stored is converted and fed to the AC supply.

The variations of the two parameters of the rectifier (viz.) the amplitude and phase of the fundamental, with respect to the mains, gives rise to a four quadrant operation. They can be stated as: leading power factor rectifier, lagging power factor rectifier, leading power factor inverter, and lagging power factor inverter (Fig. 4)(Rodriguez *et al*, 2005).

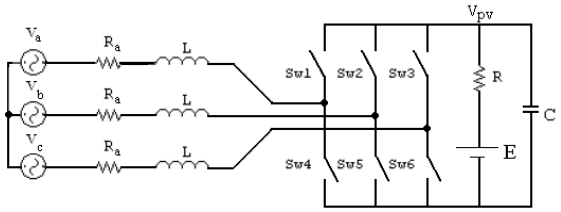

Fig. 3: Schematic diagram of the grid connected PV system.

The diodes are kept in blocked state by ensuring that DC link voltage is always higher than the peak DC voltage generated by the diodes. Failure of which diodes conduct to make the PWM rectifier behave like a common diode bridge rectifier.

Thus the diodes remain polarized negatively, and will only conduct when at least one device is switched ON, and favourable instantaneous AC voltage conditions are given. The modelled PV cell along with MPPT control is integrated to grid through a three phase PWM rectifier model.

The general simulink model of three phase PWM rectifier is obtained from its differential equation form (Rusong Wu *et al*, 1900 and 1991). The equations that had been developed considering three phase output currents and capacitor voltage as state variables are

$$\frac{di_a}{dt} = \frac{1}{L}V_a - \frac{i_a R_a}{L} - \frac{V_{PV}}{L}\left(u_1 - \frac{u_1 + u_2 + u_3}{3}\right) \quad (6)$$

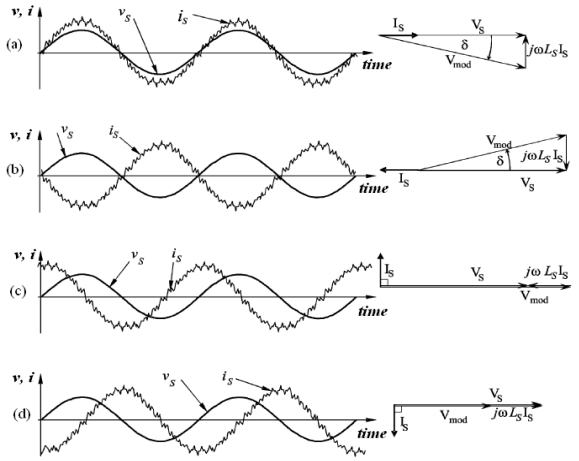

Fig. 4: Four Quadrant operation of PWM rectifier (a) Rectifier at UPF, (b) Inverter at UPF (c) Capacitor (ZPF) (d) Inductor (ZPF).

$$\frac{di_b}{dt} = \frac{1}{L}V_b - \frac{i_b R_a}{L} - \frac{V_{PV}}{L}\left(u_2 - \frac{u_1 + u_2 + u_3}{3}\right) \tag{7}$$

$$\frac{di_c}{dt} = \frac{1}{L}V_c - \frac{i_c R_a}{L} - \frac{V_{PV}}{L}\left(u_3 - \frac{u_1 + u_2 + u_3}{3}\right) \tag{8}$$

$$\frac{dV_{PV}}{dt} = \frac{1}{2C}(i_a u_1 + i_b u_2 + i_c u_3) - \left(\frac{V_{PV} - E}{RC}\right) \tag{9}$$

$$i_{PV} = \left(\frac{E - V_{PV}}{RC}\right) \tag{10}$$

where u_1, u_2 and u_3 are the switching functions of the PWM inverter defined by
u = 1; S_{w1} or S_{w3} or S_{w5} be turned ON
u = -1; S_{w2} or S_{w4} or S_{w6} be turned ON
V_{pv} is the output voltage of PV panel and ia, ib and ic are the output currents from the inverter. The state space matrix for the above equations can be represented as

$$Z\dot{x} = Ax + Bu \tag{11}$$

$$\begin{pmatrix} L & 0 & 0 & 0 \\ 0 & L & 0 & 0 \\ 0 & 0 & L & 0 \\ 0 & 0 & 0 & 2C \end{pmatrix} \begin{pmatrix} \frac{di_a}{dt} \\ \frac{di_b}{dt} \\ \frac{di_c}{dt} \\ \frac{dv_{PV}}{dt} \end{pmatrix} = \begin{pmatrix} -R & 0 & 0 & -\left(u_1 - \frac{1}{3}(u_1+u_2+u_3)\right) \\ 0 & -R & 0 & -\left(u_2 - \frac{1}{3}(u_1+u_2+u_3)\right) \\ 0 & 0 & -R & -\left(u_3 - \frac{1}{3}(u_1+u_2+u_3)\right) \\ u_1 & u_2 & u_3 & -\left(\frac{1}{R}\right) \end{pmatrix} \begin{pmatrix} i_a \\ i_b \\ i_c \\ v_{PV} \end{pmatrix} + \begin{pmatrix} 1 & 0 & 0 & 0 \\ 0 & 1 & 0 & 0 \\ 0 & 0 & 1 & 0 \\ 0 & 0 & 0 & \frac{1}{R} \end{pmatrix} \begin{pmatrix} v_a \\ v_b \\ v_c \\ E \end{pmatrix} \tag{12}$$

The modeling equations for grid are developed in such a way that any load connected to the system is supplied both from the PV source and the grid. In this paper E=0.

C. Perturb and Observe Algorithm:

Many MPPT techniques for PV systems are well established in the literature (Esram *et al*, 2007). The most commonly known method perturb and observe (P&O) is dealt with in this work. In this algorithm a slight perturbation is introduced in to the system due which the power of the module changes. The perturbation is made additive in one direction if the difference in power at the two instants is negative. The peak power is said to be obtained when further perturbation causes the difference in power at the two instants to turn positive.

The steady state is reached when the algorithm oscillates around the peak power point and hence to keep the variation in power at minimum the perturbation size has to be kept very small. The algorithm used in this paper introduces perturbation in the reference voltage of the dc-link voltage and the value corresponding to the peak power forms the corresponding voltage reference for the module.

A PI controller of the external voltage loop then acts moving the operating point of the module to that particular voltage level. The main disadvantage of this algorithm is, not stable in tracking peak power under fast varying atmospheric conditions but most widely used for its simplicity in implementation.

Once MPP, $V_{ref} = V_{pv\text{-}ref}$ is reached, operation of PV array is maintained at the point unless change in power is noted, indicating change in atmospheric conditions and the MPP (Esram *et al*, 2007). The algorithm decrements or increments V_{ref} back to new MPP. The flowchart shown in Fig. 5 represents the operation of perturb and observe algorithm.

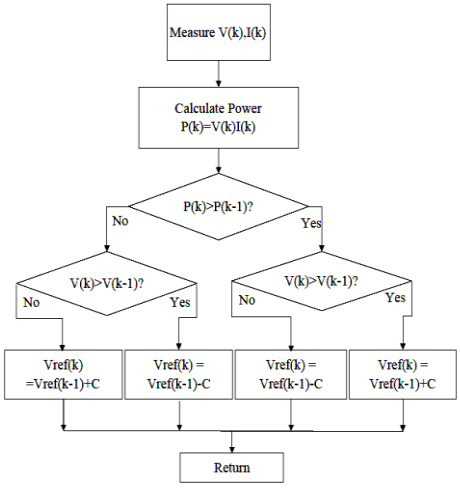

Fig. 5: Flow chart for the MPPT algorithm.

For the above proposed MPPT algorithm, a simulink model for PV has been developed by incorporating the characteristics of PV module and MPPT in MATLAB. Simulation results are obtained by varying irradiation (G), temperature (T) respectively.

D. Simulation Results for MPPT:

Fig. 6 & 7 represents the operating point of PV for maximum power output, when there is a change in solar irradiation (G), temperature (T). It is found that any increase in voltage or current beyond the maximum power point results in substantial reduction of PV output power. This necessitates operating the boost converter at Maximum Power output from the PV source.

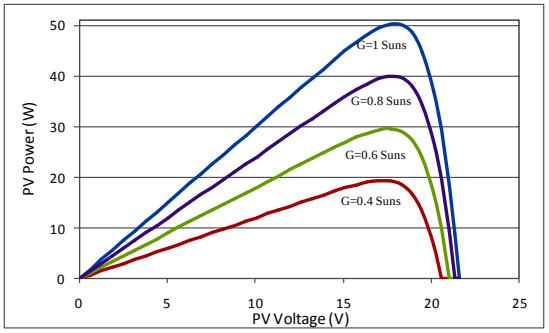

Fig. 6: MPPT for various irradiation levels (QC50, G= 0.4, 0.6, 0.8, 1 Suns, T=250C, n=1).

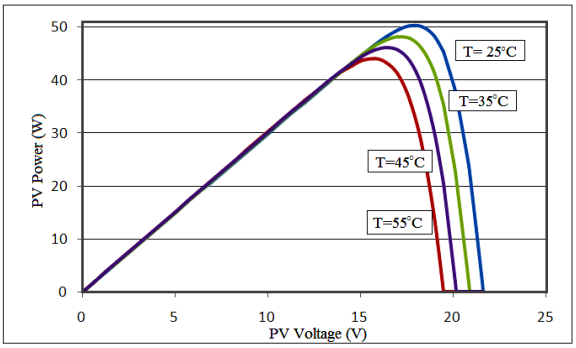

Fig. 7: MPPT for various temperatures (QC50, T= 25, 35, 45, 550C, G = 1 Suns, n=1).

E. Control Strategy for PWM Rectifier:

The control strategy for PV system is shown in Fig. 8. The MPPT algorithm chosen is the Perturb & Observe that gives the reference DC voltage which is compared to the actual DC voltage and the error is input to a PI controller. The output of the PI controller is magnitude for reference current, which is multiplied with the phase information from the source voltage to obtain reference currents I_{ref} for each phase. These reference currents are compared with the actual current of the PWM rectifier and fed to a current regulator. The output of this current regulator is compared to a carrier signal generating the pulses for the VSI.

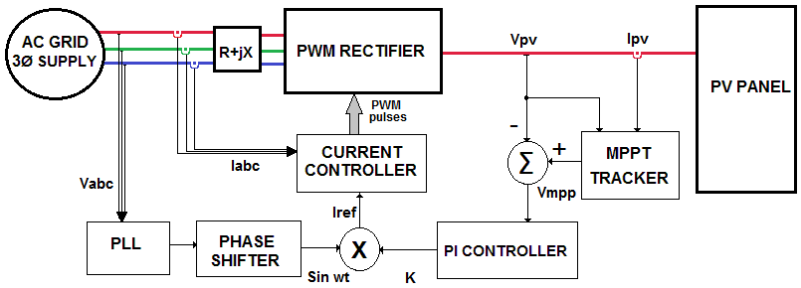

Fig. 8: Control strategy of a grid connected PV system.

Current Control Techniques:

For the schematic shown in Fig. 3, the control strategy is explained in the previous section and in this section a brief description of current control techniques is dealt with.

A. Hysteresis Controller:

The hysteresis band current control is a non linear variable switching frequency control used very often because of its simplicity of implementation. Besides fast response of the current loop, the method does not need any knowledge of load parameters. However, the current control with a fixed hysteresis band has a disadvantage, as the PWM frequency varies within a band peak-to-peak current ripple is required to be controlled at all points of the fundamental frequency wave.

The controller operates in such a way so that the actual current tracks the reference current within a hysteresis band. When the actual current crosses the upper limit of the hysteresis band, the lower switch of the inverter arm is turned on, the upper switch always complements lower switch state finally reducing current amplitude. The entire situation reverses when actual current crosses the lower limit of the hysteresis band. Here the lower switch is turned off and the upper switch is turned on, increasing the current amplitude. Eventually the actual currents operate within the hysteresis band of the current reference.

B. Sliding Mode Controller:

The SMC is a variable structure control (VSC). This technique can alter the dynamics of a nonlinear system by application of a high-frequency switching nonlinear control. A state-feedback control law derived in this case switches from one continuous structure to another based on the current position in the state space.

Multiple control structures are designed so that trajectories always move toward a switching condition, and the ultimate trajectory will slide along the boundaries of the control structures. The system is made to operate in such a way that it slides along these boundaries (sliding mode) and the geometrical locus consisting of the boundaries is called the sliding surface [18].

For the PV system considered, the current error for each phase, obtained by comparison of actual currents to respective reference currents and the differential of this current errors along with gain factors are used to form the sliding surface as given by

$$\sigma = G_1\left(I_{ref} - I_{actual}\right) + G_2\left(\dot{I_{ref}} - \dot{I_{actual}}\right) \quad (13)$$

and the control law used is

$$u=0.5(1+\mathrm{sgn}(\sigma)) \quad (14)$$

C. Linear Controller:

The inner loop current control involving transfer functions for the system in Fig. 8 using a traditional PI control is given in Fig. 9 wherein the reference currents for each phase $i_s^*(t)$ and their actual currents $i_s(t)$ are compared and used to control the converter. The conventional transfer function of PI control and PWM converter along with equations (6) to (8) is used to form the block diagram given in Fig. 9.

Australian Journal of Basic and Applied Sciences, 8(18) December 2014, Pages: 299-310

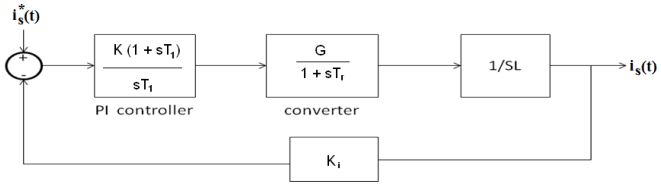

Fig. 9: Inner current control loop with PI-controller.

As seen from Fig. 9 PI controller transfer function introduces a phase lead by the T_1 element, simultaneously the converter transfer function T_r has a lag element. Now if T_1 is chosen such that it cancels the dominant lag element, T_r the system become simpler.

The response of the system for any unit step input depends on the denominator, the moment pole zero cancels the damping term is missing and the system become oscillatory. Controllers are chosen in such a way that whenever there is a variation in input the output should follow instantaneously.

But in this system, if input variation is a step, the output doesn't follow the step input as in case of first order systems, but the system can be made to act as first order system by implementing changes with a small time constant T, hence the response follow as a first order lag for any change in current.

For a first order lag, time constant T is given by

$$T\frac{di_s(t)}{dt} = \frac{i_s^*(t)}{K_i} - i_s(t) \tag{15}$$

If Vs(t) and Vr(t) represent the source voltage and inverter output voltage of a phase (refer Fig. 3) then the current across the inductor L is given by

$$V_s(t) + L\frac{di_s(t)}{dt} = V_r(t) \tag{16}$$

from equations (15) and (16) we get

$$V_r(t) - V_s(t) = \frac{L}{GTK_i}\left(i_s^*((t)) - (i_s(t)) * K_i\right) \tag{17}$$

Hence the PI controller can be replaced by a proportional (linear) controller

$$\left(\frac{L}{GTK_i}\right) \tag{18}$$

whose block diagram is shown in Fig. 10.

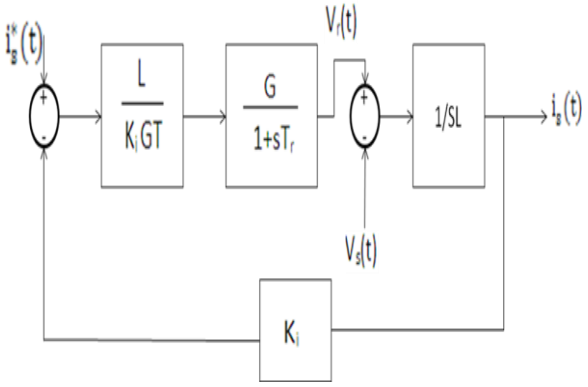

Fig. 10: Inner current control loop with linear controller.

The resulting overall transfer function of the process in Fig. 10 is a second order system given by

$$\frac{\omega_n^2}{S^2 + 2\zeta\omega_n S + \omega_n^2} \tag{19}$$

where

$$\omega_n^2 = \frac{1}{TT_r} \tag{20}$$

Australian Journal of Basic and Applied Sciences, 8(18) December 2014, Pages: 299-310

$$2\zeta\omega_n = \frac{1}{T_r} \tag{21}$$

For good response of a second order system the damping factor should be 0.707 thus resulting in

$$T=2T_r \tag{22}$$

Simulation Results:

The proposed strategy was simulated using Matlab Simulink software. The PV panel used was 50W whose specifications are given in table I. The simulation model is shown in Fig. 11.

The simulation parameters considered are

Source inductance L = 2mH,

Grid voltage = 5V RMS,

Capacitance C=220µF

DC Link Voltage =Vmpp.

Simulation results for the entire system using three current controllers are obtained by introducing a step change in PV parameters such as solar irradiation G.

Fig. 12 shows the results for Hysteresis current control technique involving (a) the three phase grid voltages and regenerative currents, (b) Individual Voltage and Current of phase A, (c) the voltage and current from the PV panel, (d) the reference voltage Vmpp output of the MPPT block for the outer voltage loop, (e) Power generated from the PV panel and Power transmitted to the grid. The response of the controller is studied by introduction of a step change in irradiation from G = 1 Suns to G =0.6 Suns at time instant t = 2.5s maintaining the temperature at 32°C.

The fact that PV output power decreases with a decrease in solar irradiation is shown in these results. Fig. 13 shows the results for sliding mode current control technique under the same operating conditions described for hysteresis current control. Fig. 14 shows the sliding surface (σ) where we see that it oscillates about the zero point. Fig. 15 shows the sliding plane and the initial trajectory moving towards error minimum.

Fig. 16 presents the results for linear current control approach for the same above said conditions.

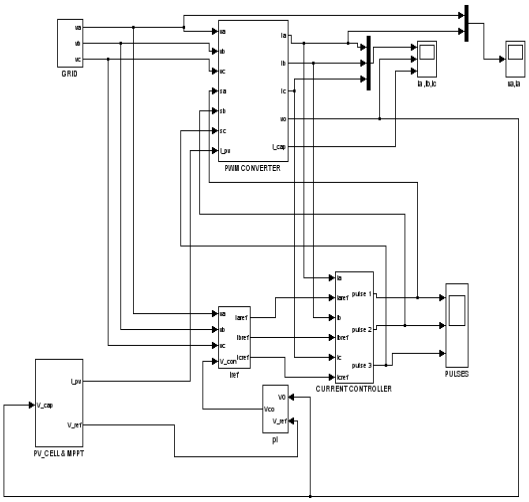

Fig. 11: Matlab Simulink Model for Single Stage PV System.

Comparative Analysis:

The Fig. 17 provides the THD profile for phase A current obtained with the three current control techniques. Table II gives the comparative analysis. As seen both hysteresis controller and sliding mode controller provides least THD compared to linear controller and all the three techniques successfully achieved UPF operation.

Table II: Comparative Analysis of three current control techniques.

Parameter	Hysteresis controller	SMC controller	Linear controller
Grid current	Sinusoidal	Sinusoidal	Sinusoidal
THD Phase (A)	6.09%	5.68%	14.12%
Power factor	UPF	UPF	UPF

Australian Journal of Basic and Applied Sciences, 8(18) December 2014, Pages: 299-310

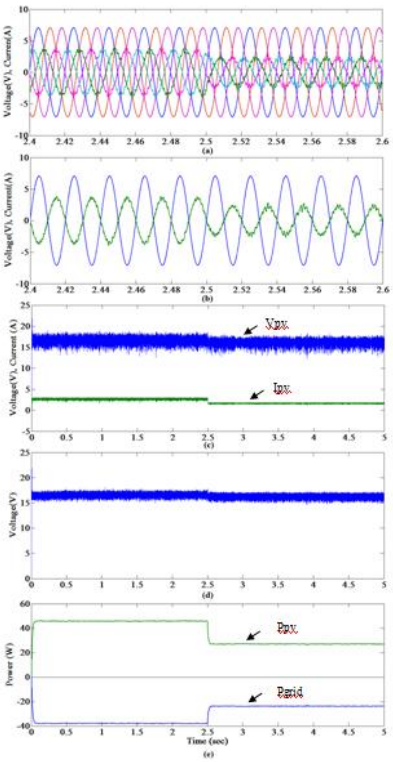

Fig. 12: Hysteresis Current Control Technique (a) Three Phase Grid Voltages and Currents (b) Voltage and Current of Phase A (c) Voltage and Current from PV Panel (d) MPPT Reference Voltage (e) Power Generated from PV Panel and Power transmitted to Grid.

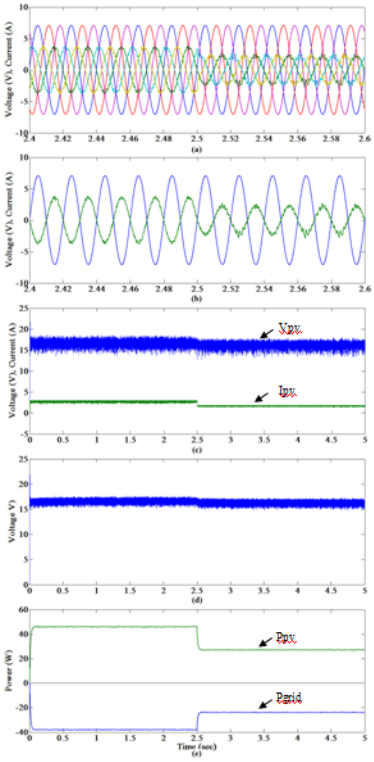

Fig. 13: Sliding Mode Current Control Technique (a) Three Phase Grid Voltages and Currents (b) Voltage and Current of Phase A (c) Voltage and Current from PV Panel (d) MPPT Reference Voltage (e) Power Generated from PV Panel and Power transmitted to Grid.

Australian Journal of Basic and Applied Sciences, 8(18) December 2014, Pages: 299-310

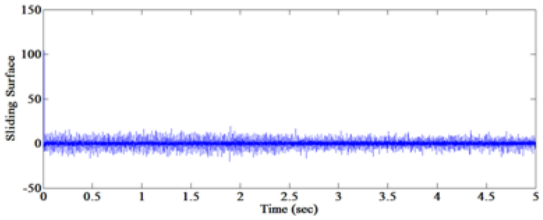

Fig. 14: Sliding Surface.

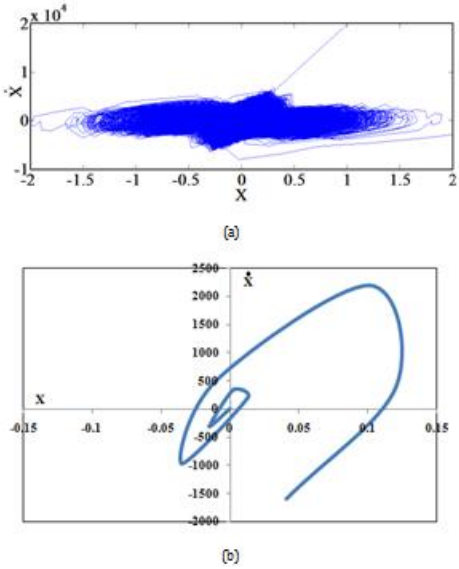

Fig. 15: (a) Sliding Plane (b) Phase Trajectory.

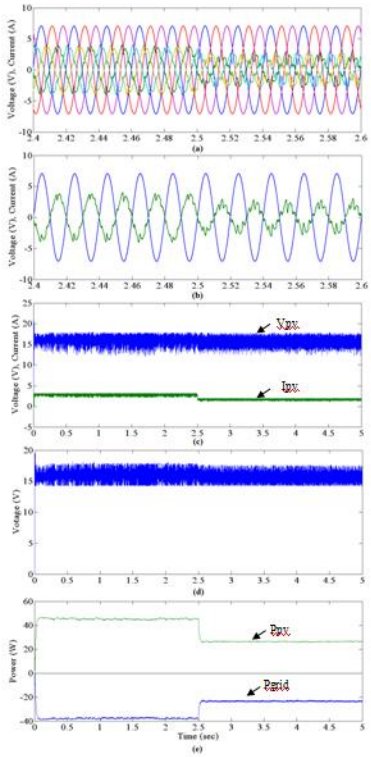

Fig. 16: Linear Current Control Technique (a) Three Phase Grid Voltages and Currents (b) Voltage and Current of Phase A (c) Voltage and Current from PV Panel (d) MPPT Reference Voltage (e) Power Generated from PV Panel and Power transmitted to Grid.

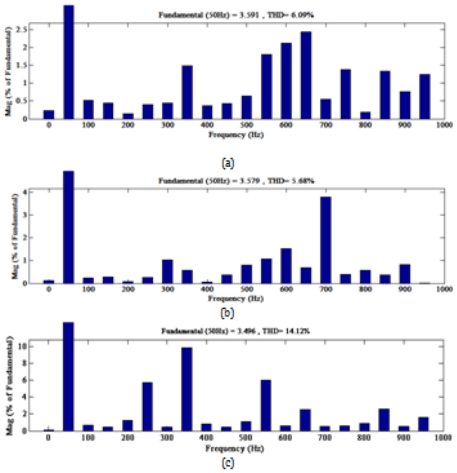

Fig. 17: THDs for Phase A Grid Current (a) Hysteresis Control (b) SMC Control (c) Linear Control.

Conclusion:

This paper dealt with grid integrated single stage solar power conversion wherein the entire system was modelled and simulated in Matlab simulink. Based on the MPPT Perturb and Observe method the maximum power is tracked from PV panel and transferred to grid at UPF and in phase opposition by using three phase PWM rectifier operating in inverse mode. The DC link voltage was controlled using a PI controller and current control loop is compared with three controllers (viz.) hysteresis current controller and sliding mode current control and linear controller. Out of the three current controllers linear controller has higher current distortion compared to others but all the three techniques successfully achieved UPF operation.

REFERENCES

Frede Blaabjerg, Zhe Chen and Soeren Baekhoej Kjaer, 2004. "Power Electronics as Efficient Interface in Dispersed Power Generation Systems", *IEEE Trans. on Power Electronics*, 19(5): 1184-1194.

Juan Manuel Carrasco, Leopoldo Garcia Franquelo, Jan T. Bialasiewicz, Eduardo Galván, Ramón C. Portillo Guisado, Ma. Ángeles Martín Prats, José Ignacio León and Narciso Moreno-Alfonso, 2006. "Power-Electronic Systems for the Grid Integration of Renewable Energy Sources: A Survey", *IEEE Trans. on Industrial Electronics*, 53(4): 1002-1016.

Yunjie Gu, Wuhua Li, Yi Zhao, Bo Yang, Chushan Li and Xiangning He, 2013. "Transformerless Inverter With Virtual DC Bus Concept for Cost-Effective Grid-Connected PV Power Systems", *IEEE Trans. on Power Electronics*, 28(27): 93-805.

Bader, N., Alajmi, Khaled, H. Ahmed, Grain Philip Adam and Barry W. Williams, 2013. "Single-Phase Single-Stage Transformer less Grid-Connected PV System", *IEEE Trans. on Power Electronics*, 28(6): 2664-2676.

Frede Blaabjerg, Remus Teodorescu, Marco Liserre and Adrian V. Timbus, 2006. "Overview of Control and Grid Synchronization for Distributed Power Generation Systems", *IEEE Trans. on Industrial Electronics*, 53(5): 1398-1409.

Wu Libo, Zhao Zhengming and Liu Jianzheng, 2007. "A Single-Stage Three-Phase Grid-Connected Photovoltaic System With Modified MPPT Method and Reactive Power Compensation", *IEEE Trans. on Energy Conversion*, 22(4): 881-886.

Mario, A., Herràn, Jonatan, R. Fischer, Sergio Alejandro Gonzàlez, Marcos G. Judewicz and Daniel O. Carrica, 2013. "Adaptive Dead-Time Compensation for Grid-Connected PWM Inverters of Single-Stage PV Systems", *IEEE Trans. on Power Electronics*, 28(6): 2816-2825.

Rodriguez, J., J. Espinoza and P. Lezana, 2005."PWM Regenerative Rectifiers: State of the Art", *IEEE Trans. on Industrial Electronics*, 52(1): 5-22.

Trishan Esram and Patrick, L. Chapman, 2007. "Comparison of photovoltaic array maximum power point tracking techniques", *IEEE Trans. on Energy Conversion*, 22(2): 439-440.

Power electronics Hand book, 2nd ed., Rashid M.H., Academic press 2001.

David Young, K., Vadim, I. Utkin and Ümit Özgüner, 1999. "A Control Engineer's Guide to Sliding Mode Control", *IEEE Trans. on Control Systems Technology*, 7(3): 328-342.

Juan José Negroni, Domingo Biel, Francesc Guinjoan and Carlos Meza, 2010."Energy-balance and Sliding Mode Control Strategies of a Cascade H-Bridge Multilevel Converter for Grid-connected PV Systems", *Proc. IEEE International Conference on Industrial Technology* (ICIT), 1155-1160.

Dannehl, J. and F.W. Fuchs, 2009. "Discrete sliding mode current control of three-phase grid-connected pwm converters," *Proc. EPE: 13th European Conference on Power Electronics and Applications* Prof., K., Gopalkumar, Lecture 12, "Design of converter control of converters", NPTEL.

Francisco, M., Gonzalez-Longatt, 2005. "Model of Photovoltaic Module in MATLAB", 2DO Congreso iberoamericano de estudiantes de ingeniería eléctrica, electrónica y Comp utación.

Rusong Wu, Sashi, B. Dewan and Gordon R. Slemon, 1990. "A PWM AC to DC Converter with fixed switching frequency", *IEEE Trans. on Industry Applications*, 26(5): 880- 885.

Rusong Wu, Sashi, B. Dewan and Gordon R. Slemon, 1991. "Analysis of an ac-to-dc Voltage Source Converter using PWM with phase and amplitude control", *IEEE Trans. on Industry Applications*.

Sliding Mode Control [Online]. Available: http://en.wikipedia.org/wiki/Sliding_mode_control.